Hindawi
Complexity
Volume 2020, Article ID 2620375, 10 pages
https://doi.org/10.1155/2020/2620375

WILEY | Hindawi

Research Article

Hyperchaotic Circuit Based on Memristor Feedback with Multistability and Symmetries

Xiaoyuan Wang,[1] **Xiaotao Min**,[1] **Pengfei Zhou**,[1] **and Dongsheng Yu**[2]

[1]*School of Electronics and Information, Hangzhou Dianzi University, Hangzhou 310018, China*
[2]*School of Electrical and Power Engineering, China University of Minning and Technology, Xuzhou 221116, China*

Correspondence should be addressed to Xiaoyuan Wang; youyuan-0213@163.com

Received 26 February 2019; Accepted 5 August 2019; Published 11 February 2020

Academic Editor: Yan-Ling Wei

A novel hyperchaotic circuit is proposed by introducing a memristor feedback in a simple Lorenz-like chaotic system. Dynamic analysis shows that it has infinite equilibrium points and multistability. Additionally, the symmetrical coexistent attractors are investigated. Further, the hyperchaotic system is implemented by analogue circuits. Corresponding experimental results are completely consistent with the theoretical analysis.

1. Introduction

Chua [1] predicted the existence of the fourth basic circuit element—memristor in 1971. However, it was not until 2008 that a team of researchers at Hewlett-Packard (HP) made nano-membrane memristive devices for the first time [2]. Since then, memristors have attracted great attentions and relative researches cover academia and industry. The emergence of memristive devices is expected to achieve nonvolatile memory. Moreover, memristors are considered to be a better way to implement artificial neural network synapses in hardware [3]. Also, due to the nonlinear characteristic of memristor, it can be used in chaotic circuits.

In 2008, Chua and Itoh [4] first constructed memristor oscillators from Chua's oscillators by replacing Chua's diodes with memristors, where the piece-wise linear (PWL) memristor model was used. Two years later, Muthuswamy [5] applied the smooth cubic flux-controlled memristor model to Chua's oscillators, which generated different chaotic attractors. The same memristor model was used in [6, 7] too. More specifically, in 2011, a twin-T notch filter was used to control chaos in a memristor based circuit in [6], and [7] implemented a hyperchaotic circuit by using this model in 2012. In 2019, based on a new current-controlled memristor, a new four-dimensional chaotic circuit is proposed and studied [8]. In these studies, nonlinear characteristic of memristor and dynamical properties of memristive chaotic and hyperchaotic circuits had been researched. In the same year, Wang presented a novel memristor model based on light dependent resistor (LDR) and its emulator in [9] and further realized a memcapacitor emulator based on the LDR memristor in [10]. Later in 2014, [11] analyzed dynamic characteristics of a LDR memristor based chaotic system. Another new memristor model was applied to Chua's circuit, and the complex transient dynamic behaviour was found in this circuit [12]. Up to now, only the HP memristor can be manufactured and widely used. In order to research application circuits with the HP memristor, [13] presented a flux-controlled model of HP memristor and analyzed its chaotic oscillator. A chaotic circuit based on two HP memristor in antiparallel was presented in [14].

The above chaotic circuits are simple and use less numbers of circuit elements. Nevertheless, there are other chaotic circuit design approaches, like Lorenz system [15], Chen system [16], Lü system [17] and most other nonlinear dynamical systems [18] could be described by ordinary differential equations containing product terms, which could easily be realized by electronic circuits via standard operational amplifiers (op-amps) and four-quadrant analogue multipliers. Generally, the op-amp is used for the integral operation and nonlinear multiplicative operation is implemented by multipliers. In this paper, the op-amps and multipliers are working together with a memristor to introduce a feedback in a chaotic circuit to realize a hyperchaotic circuit.

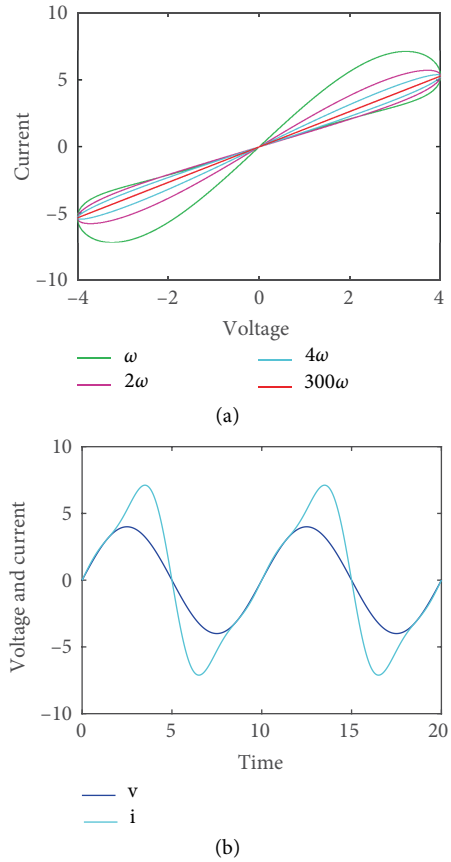

Figure 1: (a) Pinched hysteresis loop of the memristor at different frequencies. (b) Timing diagram of voltage and current.

In this paper, based on a simple chaotic circuit of three dimension Lorenz-like system, a hyperchaotic circuit was constructed by introducing a memristor feedback. This paper is organized as follows. Section 2 gives the memristor mathematical model and its equivalent circuit. In Section 3, the hyperchaotic circuit is constructed, the Lyapunov exponent and the Lyapunov dimension of the system are calculated. Section 4 discusses the stability and equilibrium points of the system. Section 5 analyzes the dynamic properties of the system, including the power spectrum and symmetrical coexistent attractors of the system. Section 6 presents the results of the circuit experiment. Section 7 draws conclusions.

2. Memristor Model and Its Equivalent Circuits

According to [19], memristors can be classified as ideal memristors, ideal generic memristors, generic memristors, and extended memristors, and the current controlled and voltage controlled ideal memristor can be described by the following relations:

$$v = R(q)i, \quad dq/dt = i, \tag{1}$$

$$i = G(\varphi)v, \quad d\varphi/dt = v, \tag{2}$$

where v and i denote the voltage cross and current goes through a memristor, q and φ are the charge and flux on the memristor at time t, $R(q)$ and $G(\varphi)$ represent memristance and memductance. A smooth flux-controlled memristor model was researched in [5], whose memductance is given by:

$$G(\varphi) = \alpha + \beta\varphi^2, \tag{3}$$

where α and β are constants and setting as $\alpha = 1$, $\beta = 0.02$ through the whole paper. Absolutely, Equation (3) describes an ideal memristor. By Matlab simulation, Figure 1(a) shows the voltage-current characteristics of the memristor at different frequencies, when it is powered by a sinusoidal voltage source, whose amplitude is chosen as 4 V and the angular frequency ω is setting to 0.1 rad/s. From Figure 1(a), we can see that the memristor degenerates into a normal resistor when the angular frequency is large enough. The time domain diagrams of voltage and current are shown in Figure 1(b). Moreover, Figure 2(a) shows the memductance of the memristor changes with time and Figure 2(b) describes the flux-charge characteristics of the memristor.

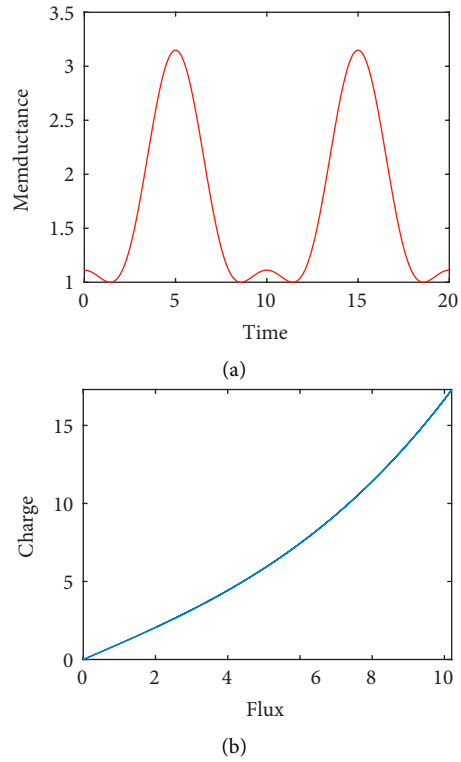

Figure 2: (a) Timing diagram of memductance. (b) Flux-charge characteristics of the memristor.

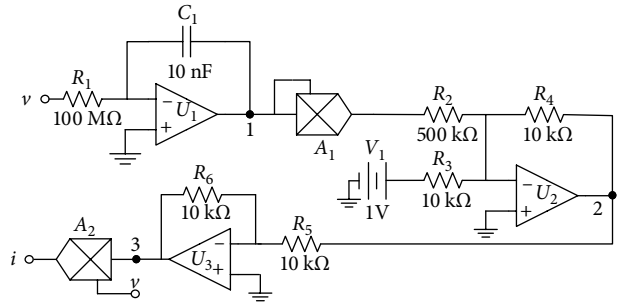

Figure 3: Equivalent circuit of the memristor.

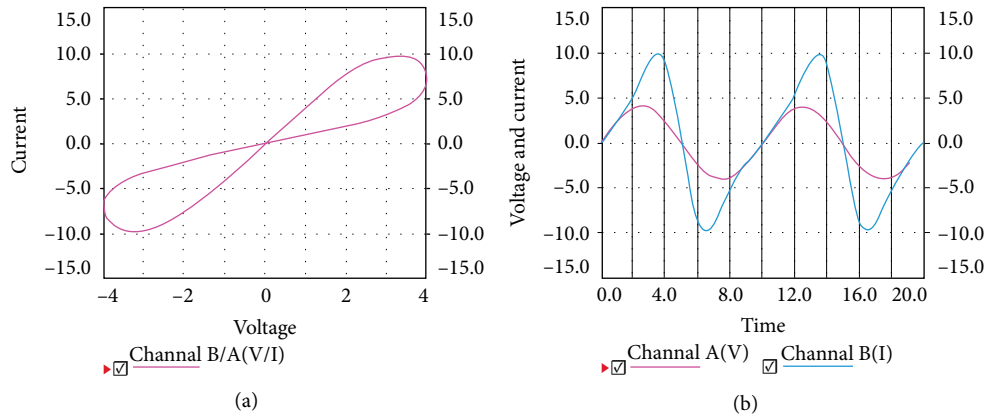

Figure 4: Simulation result of Multisim, (a) pinched hysteresis loop, and (b) timing diagram.

The emulator of the memristor described by Equation (3) is given in Figure 3. After the input voltage v passing through an integrator consisting of a resistor R_1, a capacitor C_1 and an op-amp U_1, the negative flux$(-\varphi)$ is gotten at node 1. Then φ^2 could be obtained by multiplier A_1 and the response of an inverting adder consists of resistors R_2, R_3, R_4 and op-amp U_2 can be described by the following equation:

$$-G(\varphi) = -\frac{R_4}{R_3}V_1 - \frac{R_4}{R_2}\varphi^2, \tag{4}$$

where V_1 is a DC voltage bias. The signal $-G(\varphi)$ at node 2 is inverted by the inverter composed by R_5, R_6 and op-amp U_3, then after $G(\varphi)$ at node 3 multiplying with the input voltage v in multiplier A_2, the corresponding output current i could be obtained. The Multisim simulation results of this equivalent circuit are shown in Figure 4, with input voltage $v = 4\sin(2\pi ft)$. Figure 4(a) shows the pinched hysteresis loop, the timing diagrams of voltage v and current i are shown in Figure 4(b), the results verify the effectiveness of the equivalent circuit.

3. Construction of Hyperchaotic Circuit

A simple Lorenz-like system was reported in [20], which is described as:

$$\begin{cases} \dfrac{dx}{dt} = a(y - x); \\ \dfrac{dy}{dt} = bx - xz; \\ \dfrac{dz}{dt} = x^2 - cz. \end{cases} \tag{5}$$

Such dynamical systems could easily be implemented by the op-amps and multipliers. As shown in Figure 5, if we consider the memristor as an open circuit, i.e., when the feedback has not been applied, it realizes the Lorenz-like system described by Equation (5). Now let the memristor mentioned above be used as a feedback element, according to Kirchhoff's law, basic circuit theory and the relationship between the terminal voltage and current described by Equations (2) and (3), the equivalent hyperchaotic circuit state equation in Figure 5 can be written as:

$$\begin{cases} C_1\dfrac{dv_x}{dt} = \dfrac{1}{R_2}v_y - \dfrac{1}{R_1}v_x + G(\varphi_y)v_y; \\ C_2\dfrac{dv_y}{dt} = \dfrac{1}{R_3}v_x - \dfrac{1}{R_4}v_x v_z; \\ C_3\dfrac{dv_z}{dt} = \dfrac{1}{R_5}{v_x}^2 - \dfrac{1}{R_6}v_z; \\ \dfrac{d\varphi_y}{dt} = v_y. \end{cases} \tag{6}$$

Then the dimensionless state equation of the circuit can be described by:

$$\begin{cases} \dfrac{dx}{d\tau} = a(y - x) + bG(w)y; \\ \dfrac{dy}{d\tau} = cx - xz; \\ \dfrac{dz}{d\tau} = x^2 - dz; \\ \dfrac{dw}{d\tau} = y, \end{cases} \tag{7}$$

where x, y, z and w are internal state variables of the memristive system, and a, b, c, d, α and β are parameters. When we set the parameters as $a = 24$, $b = 4$, $c = 19$, $d = 9$, $\alpha = 1$ and $\beta = 0.02$, the system can generate hyperchaos. The hyperchaotic attractor as shown in Figure 6, which indicates the hyperchaotic system has a complex dynamic behaviour. Figures 6(a)–6(d) are the hyperchaotic phase diagrams on x-y, x-z, y-z, and x-w planes, respectively. The Lyapunov exponent can be calculated as $LE_1 = 0.3399$, $LE_2 = 0.2144$, $LE_3 = -0.0045$, $LE_4 = -33.5498$ by Jacobi method, and the Lyapunov dimension D_L is 3.0164 calculated by Equation (8), which indicates that the system is hyperchaotic under the appropriate parameters.

$$D_L = j + \frac{1}{\left|LE_{j+1}\right|}\sum_{i=1}^{j} LE_i = 3 + \frac{(LE_1 + LE_2 + LE_3)}{\left|LE_4\right|}. \tag{8}$$

The expression of divergence of the memristive hyperchaotic system can be described as follows:

$$\nabla V = \frac{\partial \dot{x}}{\partial x} + \frac{\partial \dot{y}}{\partial y} + \frac{\partial \dot{z}}{\partial z} + \frac{\partial \dot{w}}{\partial w} = -a - d, \tag{9}$$

when parameters $a = 24, b = 4, c = 19, d = 9$, the ∇V is less than 0, so the system is dissipative and converge exponentially.

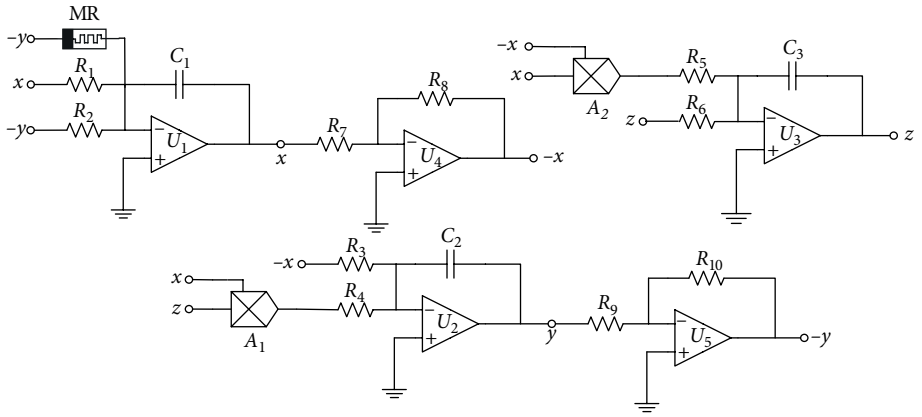

FIGURE 5: Hyperchaotic circuit by introducing memristor feedback.

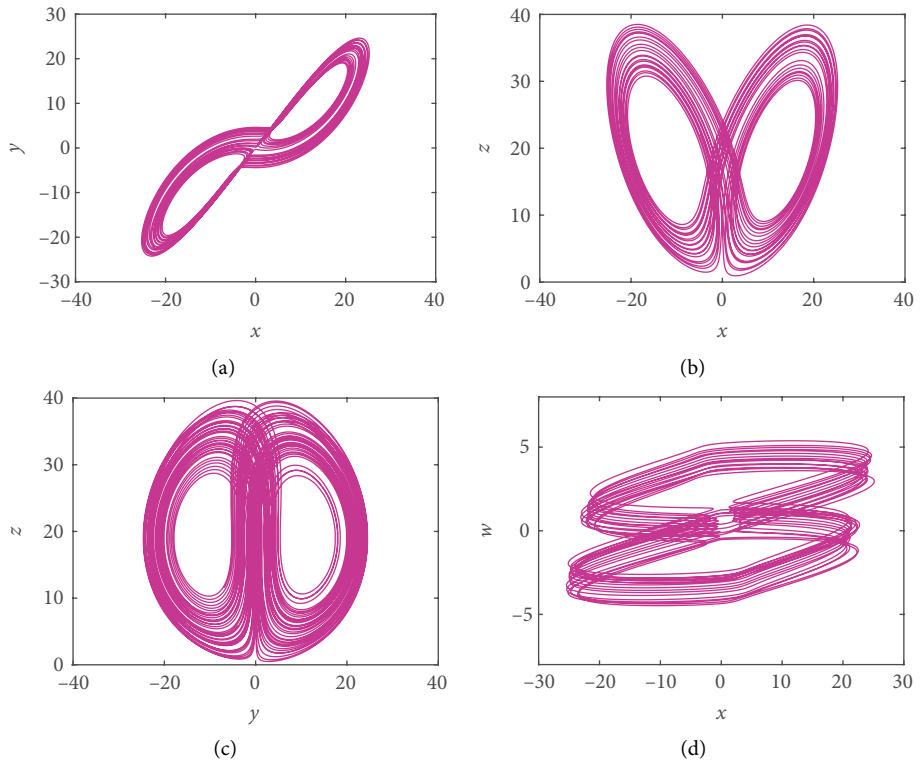

FIGURE 6: Hyperchaotic circuit by introducing memristor feedback.

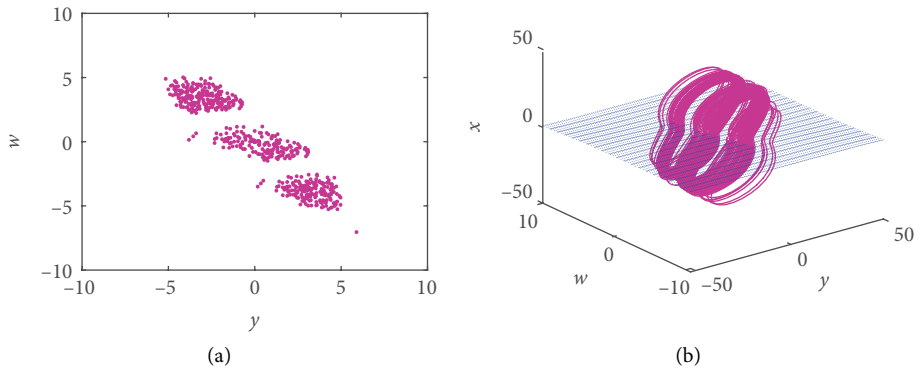

FIGURE 7: (a) Poincaré mapping projected onto $y-w$ plane and (b) space diagram of Poincaré mapping.

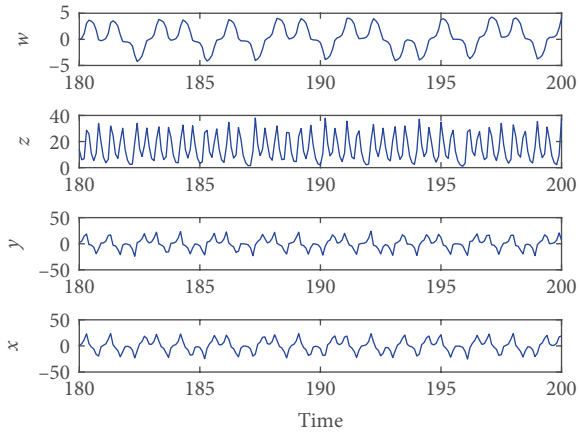

Figure 8: Time domain waveform of x, y and w.

4. Equilibrium Points and Stability of the System

In order to resolve the equilibrium of the system, let the right side of Equation (7) equal to 0, and it is found that the equilibrium points set is $O = \{x = y = z = 0, w = e\}$, which indicates that there are infinite equilibria existing in the memristive system. Different from most of the common chaotic systems, memristive chaotic systems often contain infinite equilibria points. The system's Jacobian matrix at O is described as:

$$J = \begin{bmatrix} -a & a + b\left(1 + 0.02e^2\right) & 0 & 0 \\ c & 0 & 0 & 0 \\ 0 & 0 & -d & 0 \\ 0 & 1 & 0 & 0 \end{bmatrix}. \tag{10}$$

Further, the characteristic equation corresponding to the Jacobian matrix can be obtained as follow:

$$\lambda^4 + (a + d)\lambda^3 + \left(ad - ac - bc - 0.02bce^2\right)\lambda^2 - \left(0.02bcde^2 + acd + bcd\right)\lambda = 0. \tag{11}$$

From Equation (11), the coefficients of the polynomial can be obtained, which are $a_0 = 1$, $a_1 = a + d$, $a_2 = ad - ac - bc - 0.02bce^2$, $a_3 = -\left(0.02bcde^2 + acd + bcd\right)$, $a_4 = 0$, $a_5 = 0$, $a_6 = 0$ and $a_7 = 0$. As shown in Equation (12), the coefficients of the polynomial could be arranged into a square matrix form, called the Hurwitz matrix.

$$\begin{aligned} \Delta_1 &= a_1, \\ \Delta_2 &= \begin{vmatrix} a_1 & a_3 \\ a_0 & a_2 \end{vmatrix}, \\ \Delta_3 &= \begin{vmatrix} a_1 & a_3 & a_5 \\ a_0 & a_2 & a_4 \\ 0 & a_1 & a_3 \end{vmatrix}, \\ \Delta_4 &= \begin{vmatrix} a_1 & a_3 & a_5 & a_7 \\ a_0 & a_2 & a_4 & a_6 \\ 0 & a_1 & a_3 & a_5 \\ 0 & a_0 & a_2 & a_4 \end{vmatrix}. \end{aligned} \tag{12}$$

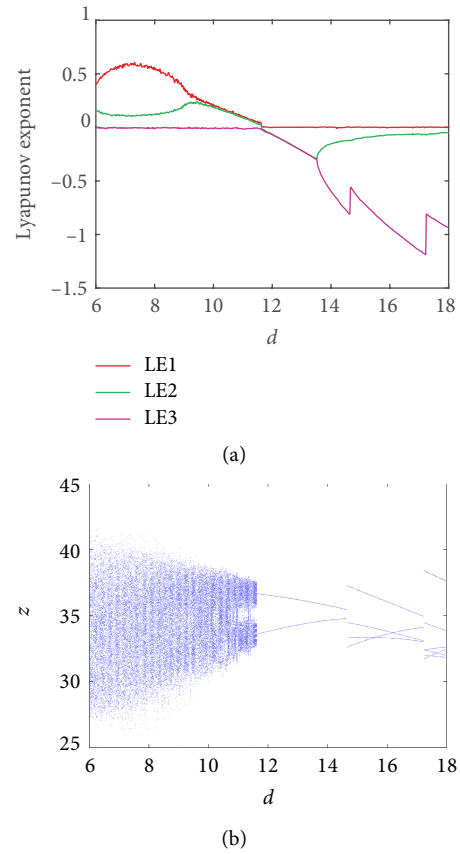

Figure 9: (a) Lyapunov exponent spectrum versus parameter d and (b) bifurcation diagram versus parameter d.

According to the Routh-Hurwitz stability criterion, the system is stable if and only if the sequences of determinants of its principal submatrices are all positive. In other words, if Δ_1, Δ_2, Δ_3 and Δ_4 are all greater than 0, then the system is stable. When parameters a, b, c, and d are set to 24, 9, 19 and 4, $\Delta_2 = -\left(912e^2\right)/25 - 5640$, which is always less than 0. So all the equilibria of the system are unstable under the above parameters, and the system may generate chaos or hyperchaos.

5. Dynamical Property Analysis

5.1. Poincaré Mapping and Sequence Diagram Analyses. When parameters are setting as $a = 24$, $b = 4$, $c = 19$, $d = 9$, the Poincaré mapping of the hyperchaotic system is shown in Figure 7. Figure 7(a) is the Poincare mapping obtained when the cross plane is selected as $x = 0$. To describe its acquisition process more vividly, Figure 7(b) shows the 3 dimensional stereoscopic graphics. Poincaré mapping reflects the motion characteristics of the system. As shown in Figure 7(a), the Poincaré mapping manifests as dense points and its structure is hierarchical, so it can be determined that the motion of the system is in a chaotic or hyperchaotic state.

Figure 8 presents the sequence diagrams of the system, which indicates the motion of the system is pseudo-random and aperiodic. So combining with the above analyses and

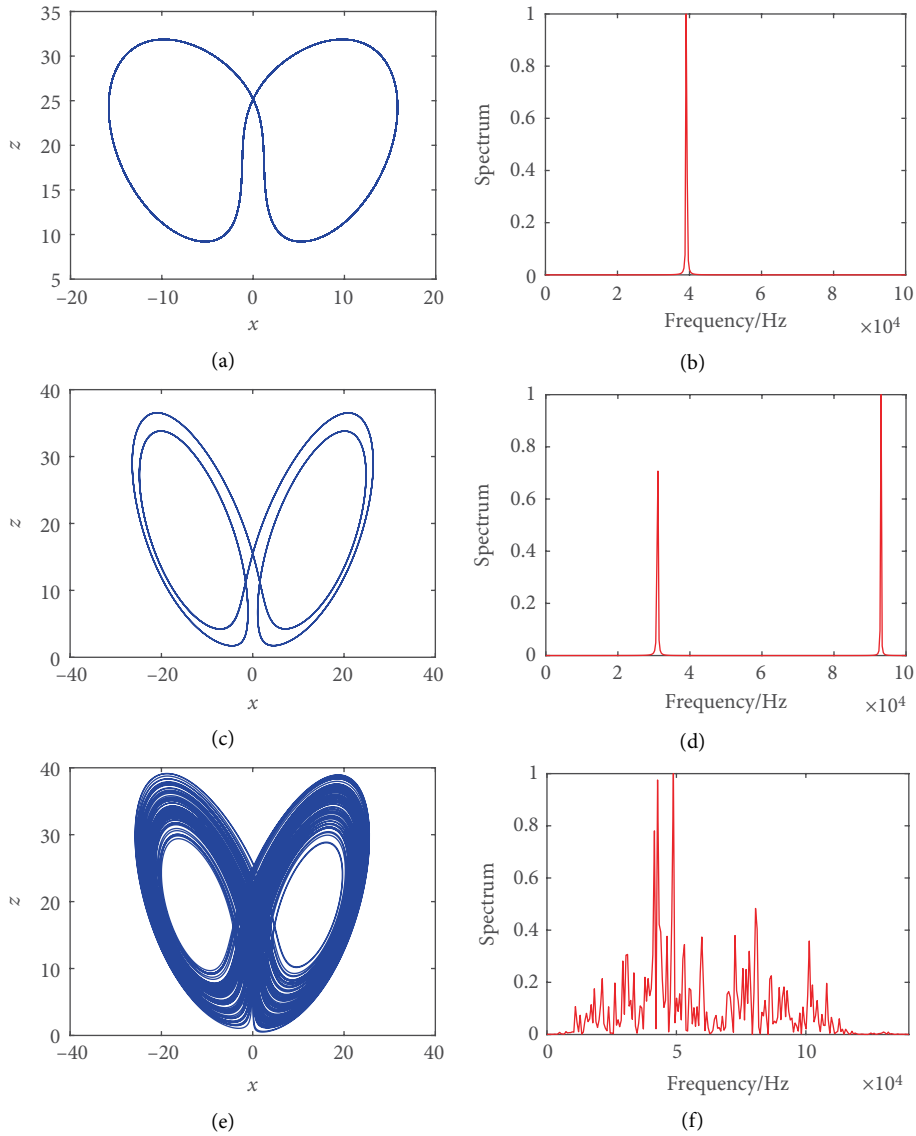

Figure 10: Attractor and power spectrum for (a, b) period-1; (c, d) period-2; (e, f) hyperchaos.

the Lyapunov exponents, it can be judged that the system could be in the hyperchaotic state under the above parameters.

5.2. Influence of Parameter Variation on Dynamics of System. Parameter variation affects the equilibrium point and stability of the system, so it is meaningful to discuss the impact of parameter changes of the system. Figure 9 shows the corresponding Lyapunov exponent spectrum and bifurcation diagram when parameter d is changing from 6 to 18, while other parameters a, b, c are fixed.

It is worth pointing out that there should be four Lyapunov exponents in a four dimension system. However, only three Lyapunov exponents are shown in Figure 9(a), because the fourth Lyapunov exponent is negative and much smaller than the other three ones, so in order to clearly show the details of the Lyapunov exponent spectrum, the fourth Lyapunov exponent is not shown. And Figure 9(b) is the corresponding bifurcation diagram, when the parameter d increases, the system gradually transitions from

Table 1: The properties of coexistent attractors under different conditions.

Properties	Parameters (a, b, c, d)	Initial values	Figure number
Symmetrical chaotic attractors	(24, 4, 2, 19)	(0, 0.1, 0, 0) (0, −0.1, 0, 0)	Figure 11(a)
Symmetrical chaotic attractors	(24, 4, 10, 19)	(0, 0.1, 0, 0.1) (0, −0.1, 0, −0.1)	Figure 11(b)
Symmetrical hyperchaotic attractors	(24, 4, 19, 9)	(0, 0.1, 0, 26) (0, −0.1, 0, −26)	Figures 11(c) and 11(d)
Symmetrical quasiperiodic attractors	(24, 4, 19, 9)	(0, 0.1, 0, 130) (0, −0.1, 0, −130)	Figure 11(e)
Symmetrical period 1 attractors	(24, 4, 19, 9)	(0, 0.1, 0, 150) (0, −0.1, 0, −150)	Figure 11(f)

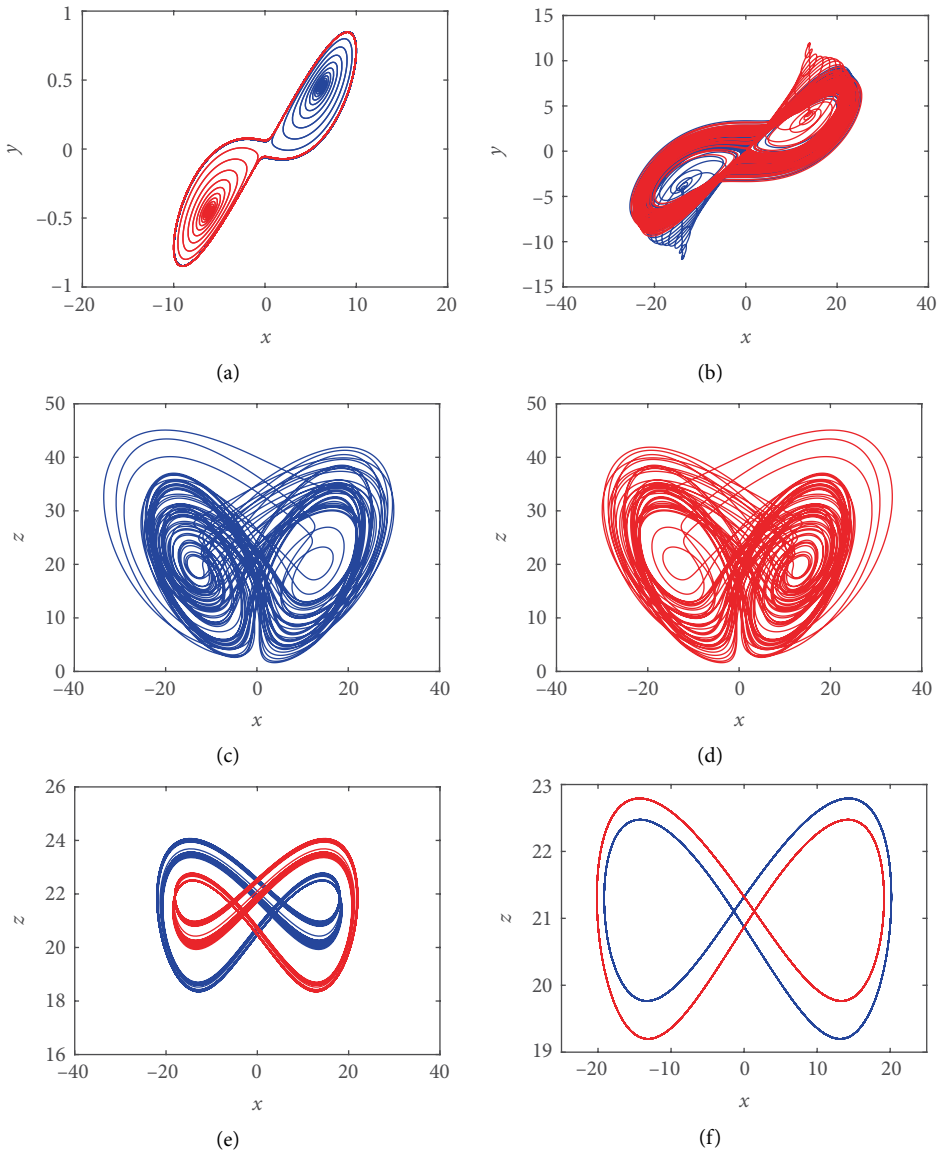

Figure 11: Symmetrical coexistent attractors of the system on the x-y, x-z plane.

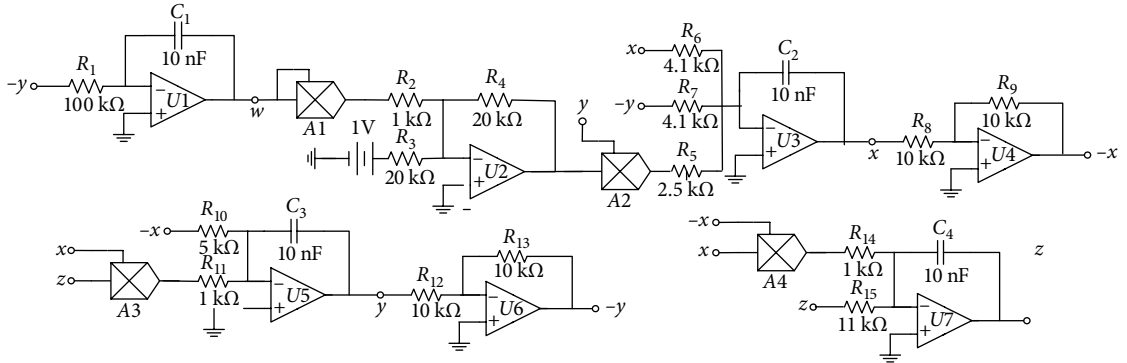

Figure 12: Circuit schematic.

hyperchaotic state to periodic state and the bifurcation diagram is consistent with the Lyapunov exponent spectrum.

Moreover, it can be clearly observed from Figure 9(a) that during d grows, there are two Lyapunov exponents greater than 0, a Lyapunov exponent equal to 0, and a Lyapunov exponent less than 0 until d reaches 11.8. This also proves that the system can indeed be in hyperchaotic state under certain parameters.

Figure 13: Chaotic attractors observed from an analog oscilloscope. (a) x-y plane; (b) x-z plane; (c) y-z plane; (d) x-w plane.

5.3. Power Spectrum Analysis. As everyone knows, the power spectrum of a periodic signal is a discrete spectrum, the power spectrum of aperiodic signals is a continuous spectrum and for a noise signal, whose power spectrum is continuous and smooth. Chaotic and hyperchaotic signals are a kind of aperiodic signal, so its power spectrum should be a continuous spectrum. Figure 10 shows the attractors and the normalized power spectrums corresponding to different states of the system. Concretely, Figure 10(a) shows period-1 attractor when parameter $d = 14.64$ and Figure 10(b) presents its sole power spectrum. Similarly, Figure 10(c) is period-2 attractor as $d = 12$ and Figure 10(d) is the corresponding discrete power spectrum. Figure 10(e) shows the hyperchaotic attractor when $d = 9$, it is worth to note that there are a large number of peaks in its corresponding power spectrum Figure 10(f). Such phenomenon is mainly due to the existence of numerous double periodic bifurcations in chaos or hyperchaos. It can be found that power spectrum analysis can be effectively used to compare and distinguish noise signals, periodic signals, chaotic and hyperchaotic signals.

5.4. Symmetrical Coexistent Attractors. The system shown in Equation (7) is symmetric about the z-axis, which can be derived from invariance when transforming (x, y, z, w) to $(-x, -y, z, -w)$, as shown in Equation (13). Therefore, the system can enter symmetrical trajectories under symmetrical initial values.

$$\begin{cases} \dfrac{dx}{d\tau} = a(y-x) \\ \qquad\quad + bG(w)y \\ \dfrac{dy}{d\tau} = cx - xz \\ \dfrac{dz}{d\tau} = x^2 - dz \\ \dfrac{dw}{d\tau} = y \end{cases} \Longleftrightarrow \begin{cases} -\dfrac{dx}{d\tau} = -a(y-x) \\ \qquad\quad + bG(w)y \\ -\dfrac{dy}{d\tau} = -cx + xz \\ \dfrac{dz}{d\tau} = x^2 - dz \\ -\dfrac{dw}{d\tau} = -y. \end{cases} \tag{13}$$

Figure 11 shows the typical coexisting attractors of this system, the blue and red trajectories are phase diagrams starting from symmetrical initial values under same sets of parameters. Table 1 presents different states and their corresponding parameters, initial values, and figure numbers in Figure 11. More specifically, in Figures 11(a) and 11(b), both of them are chaotic attractor coexisting with other symmetrical chaotic attractors. Figures 11(c) and 11(d) describe two symmetrical hyperchaotic attractors coexisting with each other. Figure 11(e) shows symmetrical quasiperiodic coexistent attractors, and symmetrical period 1 coexistent attractors are shown in Figure 11(f).

6. Circuit Experiment

From the previous analysis, the hyperchaotic system described by Equation (7) can be in hyperchaotic state when the parameters are set as $a = 24, b = 4, c = 19, d = 9, \alpha = 1$ and $\beta = 0.02$.

In order to avoid the nonlinear distortion and observe the better waveforms on the oscilloscope, the proportional compression transformation and the time scale transformation are needed to carry out on Equation (7). Let $kx \to x$, $ky \to y$, $kz \to z$ and $\tau \to t_0 t$, where $k = 10$ and $t_0 = 1000$, the system can be described as:

$$\begin{cases} \frac{dx}{dt} = 24000(y - x) + 4000\left(1 + 0.02w^2\right)y; \\ \frac{dy}{dt} = 19000x - 10000xz; \\ \frac{dz}{dt} = 10000x^2 - 9000z; \\ \frac{dw}{dt} = 1000y. \end{cases} \tag{14}$$

The designed experimental circuit is shown in Figure 12 and this circuit can be described by:

$$\begin{cases} \frac{dx}{dt} = \frac{1}{R_7C_2}y - \frac{1}{R_6C_2}x + \frac{1}{R_5C_2}\left(\frac{R_4}{R_3} + \frac{R_4}{R_2}w^2\right)y; \\ \frac{dy}{dt} = \frac{1}{R_{10}C_3}x - \frac{1}{R_{11}C_3}xz; \\ \frac{dz}{dt} = \frac{1}{R_{14}C_4}x^2 - \frac{1}{R_{15}C_4}z; \\ \frac{dw}{dt} = \frac{1}{R_1C_1}y. \end{cases} \tag{15}$$

Comparing Equation (15) with Equation (14), the corresponding circuit parameters can be determined as follows: $C_1 = C_2 = C_3 = C_4 = 10\,\text{nF}$, $R_1 = 100\,\text{k}\Omega$, $R_2 = R_{11} = R_{14} = 1\,\text{k}\Omega$, $R_3 = R_4 = 20\,\text{k}\Omega$, $R_9 = R_8 = R_{12} = R_{13} = 10\,\text{k}\Omega$, $R_5 = 2.5\,\text{k}\Omega$, $R_6 = R_7 = 4.1\,\text{k}\Omega$, $R_{10} = 5\,\text{k}\Omega$, $R_{15} = 11\,\text{k}\Omega$. The op-amp LF347 and analogue multipliers AD633 with $\pm 15\,\text{V}$ power supplies are used to construct the experimental circuit. The experimental results are shown in Figure 13, which matches well with Matlab numerical simulations shown in Figure 6.

7. Conclusions

In this paper, a hyperchaotic circuit based on memristor feedback is proposed. In addition to some conventional analysis, the frequency domain characteristics of hyperchaotic signals are analyzed by the power spectrum. Further, the infinite equilibrium points and the symmetrical coexistent attractors are found. Finally, the theoretical analysis was verified by experimental circuits.

Data Availability

The data used to support the findings of this study are available from the corresponding author upon request.

Conflicts of Interest

The authors declare that there are no conflicts of interest regarding the publication of this paper.

Acknowledgments

This work was supported by the National Natural Science Foundation of China under Grant No. 61871429, and the Natural Science Foundation of Zhejiang Province (Grant No. LY18F010012).

References

[1] L. O. Chua, "Memristor-The missing circuit element," *IEEE Transactions on Circuit Theory*, vol. 18, no. 5, pp. 507–519, 1971.

[2] D. B. Strukov, G. S. Snider, D. R. Stewart, and R. S. Williams, "The missing memristor found," *Nature*, vol. 459, no. 7250, pp. 80–83, 2008.

[3] S. H. Jo, T. Chang, I. Ebong, B. B. Bhadviya, P. Mazumder, and W. Lu, "Nanoscale memristor device as synapse in neuromorphic systems," *Nano Letters*, vol. 10, no. 4, pp. 1297–1301, 2010.

[4] M. Itoh and L. O. Chua, "Memristor oscillators," *International Journal of Bifurcation and Chaos*, vol. 18, no. 11, pp. 183–3206, 2008.

[5] B. Muthuswamy, "Implementing memristor based chaotic circuits," *International Journal of Bifurcation and Chaos*, vol. 20, no. 5, pp. 1335–1350, 2010.

[6] H. H. C. Iu, D. S. Yu, A. L. Fitch, V. Sreeram, and H. Chen, "Controlling chaos in a memristor based circuit using a twin-T notch filter," *IEEE Transactions on Circuits and Systems I: Regular Papers*, vol. 58, no. 6, pp. 1337–1344, 2011.

[7] A. L. Fitch, D. S. Yu, H. H. C. Iu, and V. Sreeram, "Hyperchaos in a memristor-based modified canonical Chua's circuit," *International Journal of Bifurcation and Chaos*, vol. 22, no. 6, p. 1250133, 2012.

[8] H. Cao and F. Wang, "Transient and steady coexisting attractors in a new memristor-based 4-D chaotic circuit," *AEU – International Journal of Electronics and Communications*, vol. 108, pp. 262–274, 2019.

[9] X. Y. Wang, A. L. Fitch, H. H. C. Iu, V. Sreeram, and V. G. Qi, "Implementation of an analogue model of a memristor based on a light-dependent resistor," *Chinese Physics B*, vol. 21, no. 10, p. 108501, 2012.

[10] X. Y. Wang, A. L. Fitch, H. H. C. Iu, and V. G. Qi, "Design of a memcapacitor emulator based on a memristor," *Physics Letters A*, vol. 376, no. 4, pp. 394–399, 2012.

[11] X. Y. Wang, G. Y. Wang, and X. Y. Wang, "Dynamic character analysis of a LDR, memristor-based chaotic system," *Journal of Circuits, Systems and Computers*, vol. 23, no. 6, p. 1450085, 2014.

[12] B. C. Bao, P. Jiang, H. G. Wu, and F. W. Hu, "Complex transient dynamics in periodically forced memristive Chua's circuit," *Nonlinear Dynamics*, vol. 79, no. 4, pp. 2333–2343, 2015.

[13] G. Y. Wang, S. C. Zang, X. W. Wang, F. Yuan, and H. H. C. Iu, "Memcapacitor model and its application in chaotic oscillator with memristor," *Chaos: An Interdisciplinary Journal of Nonlinear Science*, vol. 27, no. 1, p. 013110, 2017.

[14] A. Buscarino, L. Fortuna, M. Frasca, and L. V. Gambuzza, "A chaotic circuit based on Hewlett-Packard memristor," *Chaos: An Interdisciplinary Journal of Nonlinear Science*, vol. 22, no. 2, p. 023136, 2012.

[15] E. N. Lorenz, "Deterministic nonperiodic flow," *Journal of the Atmospheric Sciences*, vol. 20, no. 2, pp. 130–141, 1963.

[16] G. R. Chen and T. Ueta, "Yet another chaotic attractor," *International Journal of Bifurcation and Chaos*, vol. 9, no. 7, pp. 1465–1466, 1999.

[17] J. H. Lü and G. R. Chen, "A new chaotic attractor coined," *International Journal of Bifurcation and Chaos*, vol. 12, no. 3, pp. 659–666, 2002.

[18] C. Li, J. C. Sprott, T. Kapitaniak, and T. Lu, "Infinite lattice of hyperchaotic strange attractors," *Chaos, Solitons and Fractals*, vol. 109, pp. 76–82, 2018.

[19] L. O. Chua, "Everything you wish to know about memristors but are afraid to ask," *Radioengineering*, vol. 24, no. 2, pp. 319–368, 2015.

[20] C. X. Liu, T. Liu, L. Liu, and K. Liu, "A new chaotic attractor," *Chaos, Solitons and Fractals*, vol. 22, no. 5, pp. 1031–1038, 2004.